Cell Metabolism
Article

Nampt/PBEF/Visfatin Regulates Insulin Secretion in β Cells as a Systemic NAD Biosynthetic Enzyme

Javier R. Revollo,[1,9,10] Antje Körner,[6,9] Kathryn F. Mills,[1] Akiko Satoh,[1] Tao Wang,[7,8] Antje Garten,[6] Biplab Dasgupta,[2] Yo Sasaki,[2] Cynthia Wolberger,[7,8] R. Reid Townsend,[3] Jeffrey Milbrandt,[2,4,5] Wieland Kiess,[6] and Shin-ichiro Imai[1,*]

[1]Department of Molecular Biology and Pharmacology
[2]Department of Pathology
[3]Department of Medicine
[4]Department of Neurology
[5]Hope Center for Neurological Disorders
Washington University School of Medicine, St. Louis, MO 63110, USA
[6]University Hospital for Children and Adolescents, University of Leipzig, Liebigstrasse 20a, 04103 Leipzig, Germany
[7]Department of Biophysics and Biophysical Chemistry
[8]Howard Hughes Medical Institute
Johns Hopkins University School of Medicine, Baltimore, MD 21205, USA
[9]These authors contributed equally to this work.
[10]Present address: Laboratory of Signal Transduction, National Institute of Environmental Health Sciences, National Institutes of Health, Research Triangle Park, NC 27709, USA.
*Correspondence: imaishin@wustl.edu
DOI 10.1016/j.cmet.2007.09.003

SUMMARY

Intracellular nicotinamide phosphoribosyltransferase (iNampt) is an essential enzyme in the NAD biosynthetic pathway. An extracellular form of this protein (eNampt) has been reported to act as a cytokine named PBEF or an insulin-mimetic hormone named visfatin, but its physiological relevance remains controversial. Here we show that eNampt does not exert insulin-mimetic effects in vitro or in vivo but rather exhibits robust NAD biosynthetic activity. Haplodeficiency and chemical inhibition of Nampt cause defects in NAD biosynthesis and glucose-stimulated insulin secretion in pancreatic islets in vivo and in vitro. These defects are corrected by administration of nicotinamide mononucleotide (NMN), a product of the Nampt reaction. A high concentration of NMN is present in mouse plasma, and plasma eNampt and NMN levels are reduced in *Nampt* heterozygous females. Our results demonstrate that Nampt-mediated systemic NAD biosynthesis is critical for β cell function, suggesting a vital framework for the regulation of glucose homeostasis.

INTRODUCTION

Nicotinamide adenine dinucleotide (NAD) and its derivative compounds are essential coenzymes in cellular redox reactions in all living organisms. NAD also participates in a number of important signaling pathways in mammalian cells, including mono- and poly-ADP-ribosylation and synthesis of cyclic ADP-ribose and nicotinate adenine dinucleotide phosphate (Belenky et al., 2007; Rongvaux et al., 2003). Recently, it has also been demonstrated that NAD and its derivatives play an important role in transcriptional regulation (Denu, 2003; Lin and Guarente, 2003). In particular, the discovery that the evolutionarily conserved Sir2 family catalyzes protein deacetylation in an NAD-dependent manner (Imai et al., 2000; Landry et al., 2000; Smith et al., 2000) has drawn much attention to this novel role for NAD. Despite the importance of NAD in these biological events, the regulation of NAD biosynthesis in vertebrates remains poorly understood.

In prokaryotes and lower eukaryotes, such as yeast, NAD is synthesized by the de novo pathway via quinolinic acid and by the salvage pathway via nicotinic acid (Belenky et al., 2007; Revollo et al., 2007; Rongvaux et al., 2003) (see Figure S1A in the Supplemental Data available with this article online). In vertebrates, NAD biosynthesis is markedly different from that in yeast and invertebrates. Mammals predominantly use nicotinamide rather than nicotinic acid as a precursor for NAD biosynthesis (Magni et al., 1999). Instead of undergoing deamidation to nicotinic acid, nicotinamide is directly converted to nicotinamide mononucleotide (NMN) by nicotinamide phosphoribosyltransferase (Nampt) (Figures S1B and S1C). NMN is then converted to NAD by nicotinamide/nicotinic acid mononucleotide adenylyltransferase (Nmnat).

Nampt has ancient origins as an NAD biosynthetic enzyme. It was originally identified as the product of the *NadV* gene in *Haemophilus ducreyi* (Martin et al., 2001) and has been found even in some bacteriophages (Miller et al., 2003). The homology of Nampt proteins between bacteriophages, bacteria, and vertebrates is unusually high (Revollo et al., 2004; Rongvaux et al., 2003). We and other groups have characterized the biochemical nature of mammalian Nampt (Revollo et al., 2004; Rongvaux et al., 2002; van der Veer et al., 2005). We have

demonstrated that it is the rate-limiting component in the NAD biosynthetic pathway from nicotinamide and regulates the activity of the NAD-dependent deacetylase Sirt1 in mammalian cells (Revollo et al., 2004). Furthermore, we and other groups have recently determined crystal structures of the Nampt apoenzyme, the Nampt-NMN complex, and the complex of Nampt and its potent chemical inhibitor FK866 (Khan et al., 2006; Kim et al., 2006; Wang et al., 2006), demonstrating that this enzyme is a dimeric type II phosphoribosyltransferase. These studies have firmly established the biochemical and structural basis of Nampt as an NAD biosynthetic enzyme.

Interestingly, the gene encoding human Nampt was originally isolated as a presumptive cytokine named pre-B cell colony-enhancing factor (PBEF) that enhances the maturation of B cell precursors in the presence of interleukin-7 (IL-7) and stem cell factor (SCF) (Samal et al., 1994). Although this function of PBEF has not been reconfirmed to date, several groups have since reported a cytokine-like function of PBEF (Jia et al., 2004; Moschen et al., 2007; Ognjanovic and Bryant-Greenwood, 2002; Ye et al., 2005). Additionally, Nampt/PBEF has recently been reidentified as a "new visceral fat-derived hormone" named visfatin (Fukuhara et al., 2005). Strikingly, visfatin was reported to exert insulin-mimetic effects in cultured cells and to lower plasma glucose levels in mice by binding to and activating the insulin receptor. However, the physiological relevance of visfatin remains controversial (Arner, 2006; Revollo et al., 2007; Sethi, 2007; Stephens and Vidal-Puig, 2006). Subsequent studies have produced conflicting results regarding a possible connection of visfatin to obesity, type 2 diabetes, and other metabolic complications (for review, see Sethi, 2007; Stephens and Vidal-Puig, 2006). Additionally, because this protein lacks a signal sequence for secretion, it has been suggested that the presence of Nampt/PBEF/visfatin in extracellular compartments might be simply due to either cell lysis or cell death (Hug and Lodish, 2005; Stephens and Vidal-Puig, 2006).

Here we show that Nampt/PBEF/visfatin functions as an intra- and extracellular NAD biosynthetic enzyme. Therefore, we will refer to this protein primarily as Nampt throughout the rest of this paper. The extracellular form of Nampt (eNampt), which is positively secreted through a nonclassical secretory pathway, does not show insulin-mimetic effects in vitro or in vivo but rather exhibits robust, even higher, NAD biosynthetic activity compared to its intracellular form (iNampt). *Nampt*-deficient heterozygous (*Nampt*$^{+/-}$) female mice show moderately impaired glucose tolerance and reduced glucose-stimulated insulin secretion (GSIS). Consistent with this in vivo phenotype, primary islets isolated from *Nampt*$^{+/-}$ mice show significant decreases in NAD biosynthesis and insulin secretion in response to glucose. A similar phenotype is also observed in wild-type primary islets treated with FK866. These defects in NAD biosynthesis and GSIS can be corrected by the administration of the Nampt reaction product NMN in vivo and in vitro, demonstrating that the observed defects are due to the lack of the NAD biosynthetic activity of Nampt. Strikingly, a high concentration of NMN is found in mouse plasma, and plasma eNampt and NMN levels are reduced in *Nampt*$^{+/-}$ females. These findings strongly suggest that Nampt-mediated systemic NAD biosynthesis plays a critical role in the regulation of β cell function, providing important insights toward developing preventive/therapeutic interventions against metabolic complications such as type 2 diabetes.

RESULTS

Nampt Is Highly Expressed in Brown Adipose Tissue, Liver, Kidney, and Heart in Mice

It has been shown that Nampt has both intra- and extracellular forms in mammals, but their physiological functions have been the matter of debate (Revollo et al., 2007). To elucidate the physiological role of Nampt, we first surveyed the tissue distribution of iNampt in mice (Figure 1A). Among the tissues examined, brown adipose tissue (BAT), liver, and kidney showed the highest levels of iNampt protein expression, and heart showed an intermediate level of iNampt. White adipose tissue (WAT), lung, spleen, testis, and muscle showed low levels of iNampt, and levels of iNampt in the brain and pancreas were undetectable. These findings suggest that the requirement of Nampt-mediated NAD biosynthesis might vary widely among different tissues.

Differentiated Adipocytes Produce eNampt

Because Nampt has been reported to act as an adipokine (Fukuhara et al., 2005), we examined the production of intra- and extracellular Nampt by brown and white adipocytes. We compared iNampt and eNampt levels between the mouse preadipocyte cell lines HIB-1B and 3T3-L1, which can differentiate into brown and white adipocytes, respectively. iNampt was highly induced during the differentiation of HIB-1B cells (Figure 1B, upper panel). In parallel with this induction, we also detected increasing amounts of eNampt from day 2 to day 8 in HIB-1B conditioned medium (Figure 1B, lower panel). This immunodetectable eNampt was purified from HIB-1B conditioned medium, and its physical identity was confirmed by tandem mass spectrometric peptide analyses (data not shown). We estimated that the concentration of eNampt in HIB-1B conditioned medium at day 8 was ~100 ng/ml (data not shown), a concentration comparable to that of adiponectin in 24 hr culture supernatants of differentiated human adipocytes (Wang et al., 2005). During the differentiation of 3T3-L1 white preadipocytes, a similar induction of iNampt was detected, although the final induction level of iNampt in differentiated 3T3-L1 cells was significantly lower than that in differentiated HIB-1B cells (Figure 1C, upper panel). A very low level of eNampt was detectable in 3T3-L1 conditioned medium at day 8 after concentration (Figure 1C, middle and lower panels). iNampt protein levels also increased mildly during the differentiation of human SGBS white preadipocytes (Figure 1D, left panel). eNampt was detectable in concentrated SGBS conditioned medium at day 8 when SGBS cells fully differentiated and started secreting adiponectin (Figure 1D,

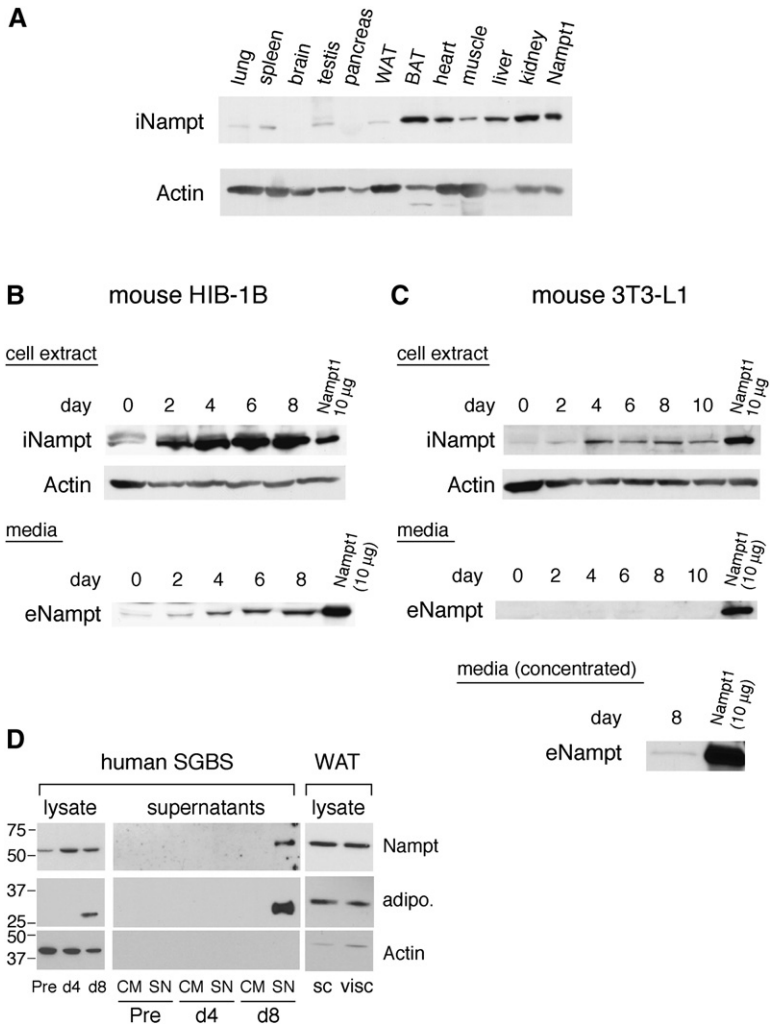

Figure 1. Tissue Distribution of Intracellular Nampt in Mice and Production of Intra- and Extracellular Nampt during Adipocyte Differentiation

(A) Distribution of intracellular Nampt (iNampt) in mouse tissues. 22.5 μg of each tissue extract from a C57BL/6 mouse was analyzed by western blotting with Nampt- and actin-specific antibodies; 5 μg of cell extract from a Nampt-overexpressing NIH 3T3 cell line (Nampt1) was loaded as a reference. WAT, white adipose tissue; BAT, brown adipose tissue.

(B) Production of intra- and extracellular Nampt (iNampt and eNampt) during differentiation of HIB-1B brown preadipocytes. Upper panel: Confluent cultures of HIB-1B cells were differentiated, and cell extracts were prepared at the indicated days. Forty-five micrograms of each cell extract was analyzed. Lower panel: 20 μl of each culture supernatant collected at the indicated days was analyzed.

(C) Production of iNampt and eNampt during differentiation of 3T3-L1 white preadipocytes. Upper panel: 45 μg of each cell extract collected at the indicated days was analyzed. Middle panel: 20 μl of culture supernatant was analyzed. Lower panel: Concentrated culture supernatant was analyzed at day 8 to detect eNampt. Ten micrograms of cell extract from Nampt-overexpressing fibroblasts (Nampt1) was loaded as a reference in each experiment.

(D) Production of iNampt and eNampt during differentiation of human SGBS white preadipocytes. Left and middle panels: 13 μg of each cell extract and 25 μl of each culture supernatant (10-fold concentrated) collected at the indicated points were analyzed. Adiponectin production is also shown as a positive control for adipocyte differentiation. Pre, undifferentiated preadipocytes; d4, differentiating adipocytes at day 4; d8, mature adipocytes; CM, control medium; SN, supernatant. Right panel: iNampt protein expression was analyzed in tissue extracts from human subcutaneous (sc) and visceral (visc) WAT.

middle panel). iNampt protein expression was also confirmed in human subcutaneous and visceral WAT extracts (Figure 1D, right panel).

We further examined whether other cell types are capable of producing eNampt. We examined NIH 3T3 (a mouse fibroblast cell line), HEK293 (a human embryonic kidney cell line), Hepa1-6 (a mouse hepatocyte cell line), COS-7 (a SV40-transformed monkey kidney cell line), and chinese hamster ovary (CHO) cells. None of these cell lines naturally produced eNampt; however, detectable amounts of eNampt were observed in conditioned media from COS-7 and CHO cells when Nampt was highly overexpressed (data not shown). Thus, eNampt is produced in a cell-type-dependent manner, suggesting that eNampt secretion is a highly regulated process. In this regard, HIB-1B cells, which can produce high levels of both iNampt and eNampt, provide a useful, robust culture system to further investigate the production and function of eNampt.

eNampt Is Positively Secreted through a Nonclassical Secretory Pathway

It has been speculated that the apparent "secretion" of eNampt might be simply due to either cell lysis or cell death (Hug and Lodish, 2005; Stephens and Vidal-Puig, 2006). We therefore investigated whether the production of eNampt is due to positive secretion or to cell lysis/death. We constructed C-terminally FLAG-tagged versions of Nampt (Nampt-FLAG) as well as dihydrofolate reductase (Dhfr) and preprolactin (Ppl) as controls for intracellular and extracellular proteins, respectively (Dhfr-FLAG and Ppl-FLAG). HIB-1B cell lines that stably expressed these FLAG-tagged proteins were established and differentiated. Dhfr-FLAG was detected exclusively in cell extracts (Figure S2A), whereas prolactin-FLAG (Prl-FLAG) was detected predominantly in supernatants (Figure S2B). Significant levels of Nampt-FLAG were detected in both cell extracts and supernatants in these cell lines, demonstrating

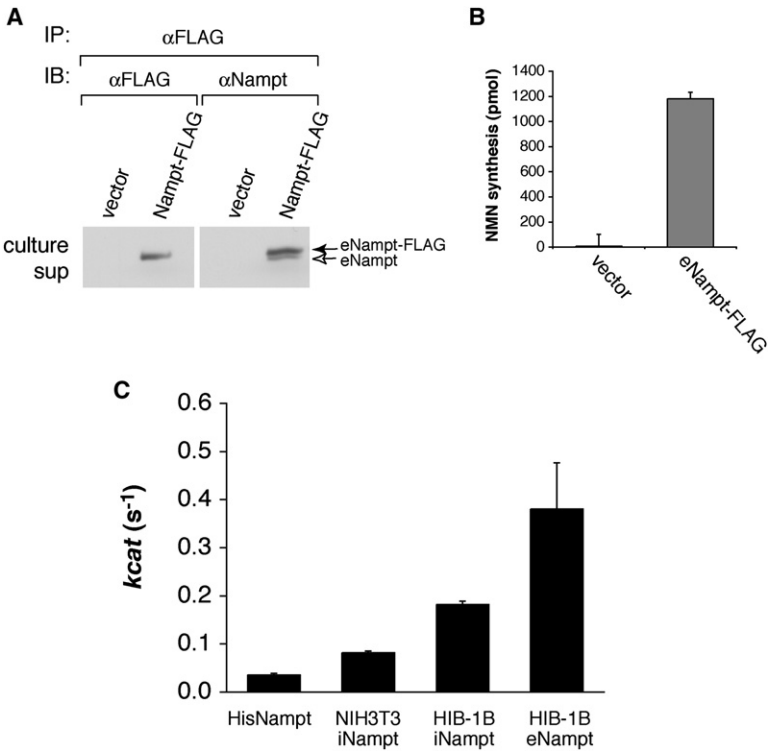

Figure 2. eNampt Produced by Differentiated HIB-1B Brown Adipocytes Has High Nampt Enzymatic Activity

(A) eNampt-FLAG coimmunoprecipitates with untagged eNampt from culture supernatants. The eNampt-FLAG protein was immunoprecipitated with an anti-FLAG antibody from 8 ml of each culture supernatant and blotted with either the same antibody or an anti-Nampt antibody. The culture supernatants of the vector-transfected cells were used as a control.

(B) eNampt-FLAG protein immunoprecipitated from culture supernatants of differentiated Nampt-FLAG HIB-1B cells has Nampt enzymatic activity. Results are presented as mean ± SEM (n = 3).

(C) The k_{cat} values of bacterially produced His-tagged recombinant Nampt and intra- and extracellular Nampt-FLAG from NIH 3T3 cells and differentiated HIB-1B cells were calculated by measuring nicotinamide mononucleotide (NMN) synthesis and quantifying the amount of Nampt by western blotting (data not shown). Results are presented as mean ± SEM (n = 7 for His-tagged Nampt, 3 for iNampt from NIH 3T3, 6 for iNampt from HIB-1B, and 4 for eNampt from HIB-1B); all differences in pairwise comparisons are statistically significant by Student's t test ($p < 0.05$).

that the presence of eNampt in supernatants is not due to cell lysis or cell death. We also treated these cell lines with brefeldin A (BFA), an inhibitor of protein secretion through the Golgi-ER system. While eNampt-FLAG levels in the supernatant were not affected by BFA, the secretion of Prl-FLAG was significantly inhibited by BFA (Figure S2C). This finding suggests that eNampt is not secreted through a classical Golgi-ER system but rather through a nonclassical secretory pathway. We achieved similar results by transfecting CHO cells with each of the FLAG-tagged constructs (data not shown). These results demonstrate that specific cell types (adipocytes and CHO cells) positively secrete eNampt through a nonclassical secretory pathway.

eNampt Produced by Differentiated Adipocytes Is Enzymatically Active

Using differentiated HIB-1B brown adipocytes as a model system, we next analyzed the enzymatic activities of iNampt and eNampt. Interestingly, we noticed that untagged eNampt coimmunoprecipitated with eNampt-FLAG (Figure 2A), indicating that eNampt forms a dimer, as observed in the crystal structure (Wang et al., 2006). The dimer formation of Nampt was also confirmed as an ~100 kDa peak by size exclusion chromatography (Figure S3). To examine whether dimerization is necessary for Nampt enzymatic activity, we mutated Ser199 and Ser200, both of which play key roles in forming a symmetrical dimer interface (Wang et al., 2006; Figure S3A), to aspartic acid. The S199D and S200D Nampt mutants do not dimerize properly and show decreased enzymatic activity (Figure S3B; Table S1), suggesting that dimerization is important for Nampt enzymatic activity.

The immunoprecipitates from the HIB-1B culture supernatants were subjected to enzyme-coupled fluorometric assays (Revollo et al., 2004) to compare the enzymatic activities of iNampt and eNampt. The immunoprecipitated eNampt-FLAG protein exhibited robust activity, while immunoprecipitates from culture supernatants of the backbone vector-transfected HIB-1B cells showed no activity (Figure 2B). We also measured the Nampt enzymatic activity of the bacterially produced recombinant Nampt and the iNampt-FLAG immunoprecipitated from HIB-1B and NIH 3T3 cellular extracts and calculated their k_{cat} values. Surprisingly, the eNampt-FLAG secreted from differentiated HIB-1B cells showed a significantly higher k_{cat} value (0.380/s) than recombinant Nampt (0.035/s, ~11-fold increase), iNampt-FLAG from NIH 3T3 cells (0.082/s, ~5-fold increase), and iNampt-FLAG from differentiated HIB-1B cells (0.182/s, ~2-fold increase) (Figure 2C). Taken together, our findings provide strong evidence that Nampt functions both intra- and extracellularly as a robust, dimeric NAD biosynthetic enzyme.

eNampt Does Not Exert Insulin-Mimetic Effects In Vitro and In Vivo

Fukuhara et al. (2005) have reported that the same protein, renamed visfatin, exerts insulin-mimetic effects on cultured cells by binding to and activating the insulin receptor. Therefore, we examined whether eNampt/visfatin indeed exerts insulin-like effects.

We first investigated the potency of exogenously administered Nampt/visfatin (eNampt/visfatin) to induce adipocyte differentiation in the human SGBS preadipocyte cell line. While SGBS preadipocytes fully differentiated

into mature adipocytes in the presence of insulin (20 nM), we did not detect differentiation into mature adipocytes with equimolar concentrations of eNampt/visfatin (Figure 3A). Additionally, eNampt/visfatin proteins produced in both bacteria and mammalian cells failed to mimic insulin's ability to induce expression of adipocyte differentiation markers such as adiponectin and PPARγ (Figure 3B). We also examined whether eNampt/visfatin can enhance glucose uptake in differentiated human SGBS and mouse 3T3-L1 adipocytes. While insulin shows dose-dependent stimulation of glucose uptake, 100 nM eNampt/visfatin did not show any effect on glucose uptake in differentiated adipocytes (Figure 3C).

Because we were unable to reproduce the reported insulin-mimetic activity of visfatin for adipogenesis and glucose uptake, we next examined whether eNampt/visfatin could induce insulin signaling. In this experiment, we employed several different cell models: the human SGBS cell line; the mouse 3T3-L1 cell line that was also used in the original report of visfatin (Fukuhara et al., 2005); and R- and R-IR cells, mouse fibroblast cell lines in which the endogenous insulin-like growth factor 1 (IGF-1) receptor is disrupted (R-) but the human insulin receptor is stably overexpressed (R-IR) (Miura et al., 1995). Although insulin (10 nM) induced significant phosphorylation of the insulin receptor and the downstream signaling kinase Akt in each of these cell lines, equimolar concentrations of eNampt/visfatin failed to induce phosphorylation of either the insulin receptor or Akt (Figure 3D; Figure S4A). The dose-dependent phosphorylation of the insulin receptor was also observed in R-IR cells with 1–100 nM insulin, but 10 and 100 nM eNampt/visfatin were unable to induce phosphorylation in these cells (Figure 3E). Additionally, conditioned media prepared from either control or Nampt-overexpressing COS-7 cells did not induce phosphorylation of the insulin receptor or Akt (Figure S4B).

We also examined whether eNampt/visfatin reduces blood glucose levels in vivo. Consistent with our results from cell culture experiments, we were unable to detect any immediate decrease in blood glucose levels even when very high doses (i.e., 20-fold higher than previously reported) of recombinant Nampt were injected (Figure S4C). Thus, in contrast to the original report of visfatin (Fukuhara et al., 2005), we were unable to reproduce the insulin-mimetic function of visfatin for adipogenesis, glucose uptake, insulin signaling, or blood glucose reduction.

Nampt$^{+/-}$ Mice Show Impaired Glucose Tolerance and Reduced Glucose-Stimulated Insulin Secretion

To further elucidate the physiological role of Nampt, we generated *Nampt*-deficient mice using a 129/Ola ES cell line designated RRT307 created by the BayGenomics consortium (currently a part of the International Gene Trap Consortium; http://www.genetrap.org). In the RRT307 ES cell line, the *Nampt* gene locus is disrupted by the insertion of a β-galactosidase/neomycin (β-geo) exon-trap vector between exon 8 and exon 9. As a result of this insertion, the C-terminal 128 amino acids are truncated and an ~190 kDa fusion protein of Nampt and β-geo is produced. Because the deleted residues include critical amino acids that contribute to the Nampt catalytic site, such as Gly384 and Arg392 (Wang et al., 2006), this fusion protein is expected to be enzymatically deficient. Consistent with this notion, mice homozygous for the *Nampt* mutant allele died prior to embryonic day 10.5 (data not shown). *Nampt* heterozygous (*Nampt*$^{+/-}$) mice were overtly normal but showed significant decreases in iNampt levels in all tissues examined (heart, liver, kidney, and BAT) and expressed the Nampt-β-geo fusion protein (Figures S5A–S5D). We also measured total NAD levels in BAT and liver from *Nampt*$^{+/-}$ and control mice (Figure S5E). While NAD levels were significantly decreased to ~66% of control in *Nampt*$^{+/-}$ BAT, no significant difference was observed in NAD levels between *Nampt*$^{+/-}$ and control livers. This presumably reflects the strong contribution of the tryptophan-kynurenine pathway to de novo NAD biosynthesis in the liver (Magni et al., 2004). Interestingly, female *Nampt*$^{+/-}$ mice showed a significant decrease in plasma eNampt levels (~50% of control eNampt levels), consistent with a decrease in tissue iNampt levels, while a similar decrease was not observed in *Nampt*$^{+/-}$ males (Figure S5F).

Both male and female *Nampt*$^{+/-}$ mice showed normal body weight and mostly normal fed and fasted glucose levels (Figures 4A and 4B). *Nampt*$^{+/-}$ and control mice did not differ significantly in percent islet area or islet morphology (Figures S6A and S6B). However, *Nampt*$^{+/-}$ female mice showed moderately impaired glucose tolerance during intraperitoneal glucose tolerance tests (i.p. GTTs) as compared to control mice (Figure 4C), while males did not show this phenotype (Figures S6C and S6D). We also measured plasma insulin levels in female *Nampt*$^{+/-}$ and control mice during i.p. GTTs. *Nampt*$^{+/-}$ mice showed significant decreases in insulin secretion at 15 and 30 min after glucose injection compared to control littermates, consistent with the i.p. GTT results (Figure 4D). We also conducted insulin tolerance tests on these female mice, but no difference was detected between *Nampt*$^{+/-}$ and control mice (Figure 4E). These results suggest that *Nampt* haplodeficiency significantly affects GSIS in pancreatic β cells and causes impaired glucose tolerance in mice.

To confirm these in vivo results, we also examined GSIS in isolated primary islets. Wild-type primary islets had a low level of iNampt protein expression (~10-fold lower than liver), and *Nampt*$^{+/-}$ islets exhibited a significant decrease in iNampt expression (Figures S6E and S6F). Because Nampt has a K_M of 0.92 μM for nicotinamide (Revollo et al., 2004), which falls within the physiological range of plasma nicotinamide concentrations in mammals (Revollo et al., 2007), we cultured isolated primary islets overnight in RPMI medium containing 1 μM nicotinamide prior to insulin secretion experiments. Under this experimental condition, primary islets isolated from *Nampt*$^{+/-}$ female mice showed an ~40% decrease in NAD levels and a comparable decrease in GSIS compared to those from wild-type littermates (Figures 4F and 4G). Therefore, consistent with the in vivo results, these findings support the

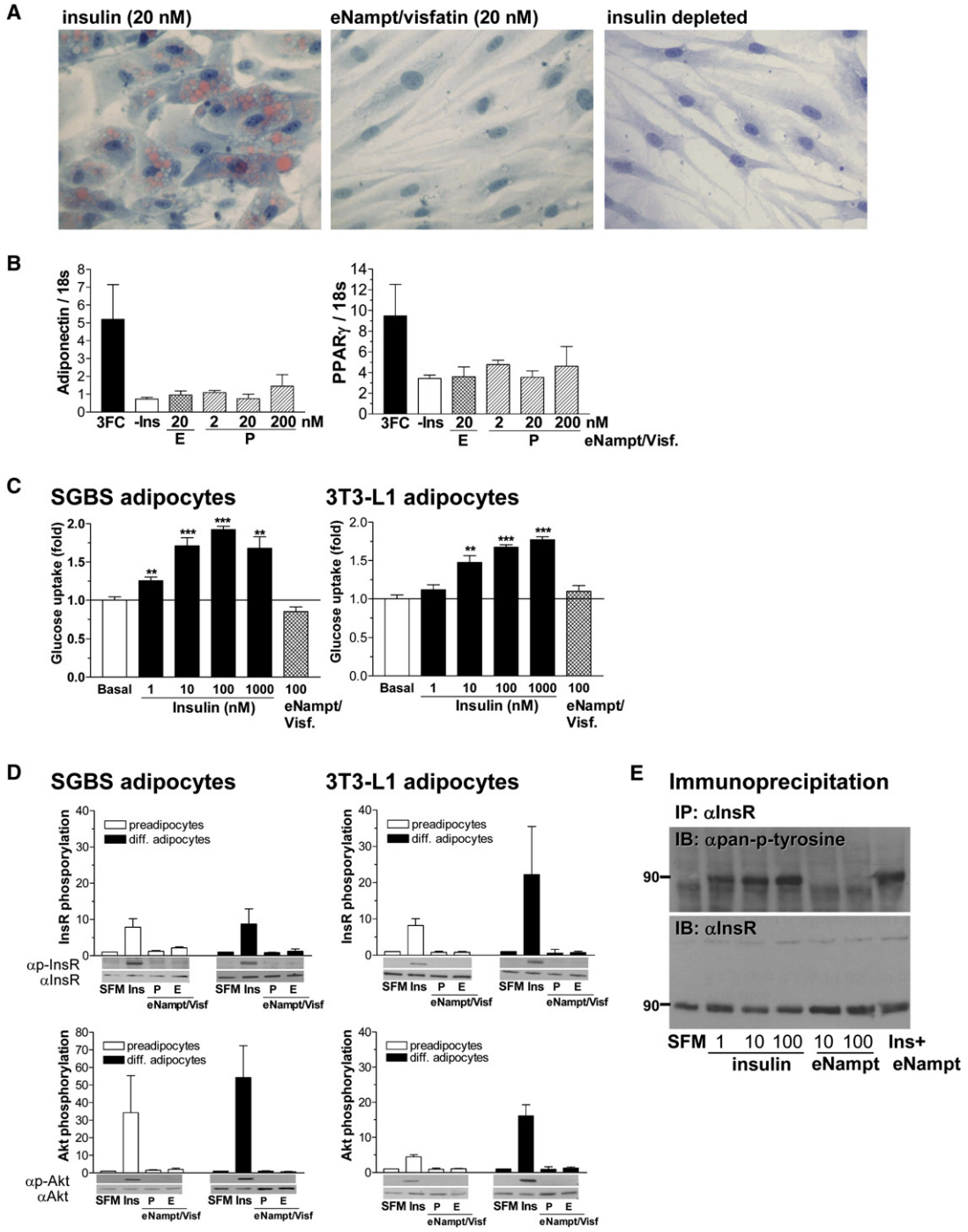

Figure 3. eNampt Does Not Exert Insulin-Mimetic Effects on Adipogenesis, Glucose Uptake, or Insulin Signaling in Cultured Cells

(A) Differentiation of human SGBS preadipocytes was induced over a period of 8 days in standard induction medium containing 20 nM insulin or 20 nM eNampt/visfatin. As a negative control, cells were treated in induction medium without insulin. Mature adipocytes were stained with Sudan III to visualize lipid accumulation at day 8.

(B) mRNA expression levels of two adipocyte differentiation markers, adiponectin and PPARγ, were analyzed by real-time quantitative RT-PCR. SGBS preadipocytes were differentiated in standard induction medium with 20 nM insulin (3FC) or eNampt/visfatin proteins produced in bacteria (P) or in mammalian cells (E) at the concentrations indicated.

(C) Differentiated SGBS and 3T3-L1 adipocytes were incubated with increasing concentrations of insulin or 100 nM eNampt/visfatin produced in mammalian cells. Glucose uptake was determined using [^{14}C]2-deoxyglucose at 0.5 μCi/ml for 5 min. Experiments were performed in quadruplicate, and glucose uptake was normalized to the amount of protein. Basal glucose uptake in nonstimulated cells was set as 1.

(D) The effect of eNampt/visfatin on phosphorylation of the insulin receptor (InsR, upper panels) and Akt/PKB kinase (Akt, lower panels) was examined in undifferentiated and differentiated human SGBS and mouse 3T3-L1 cells. Cells were starved overnight and then exposed to serum-free medium

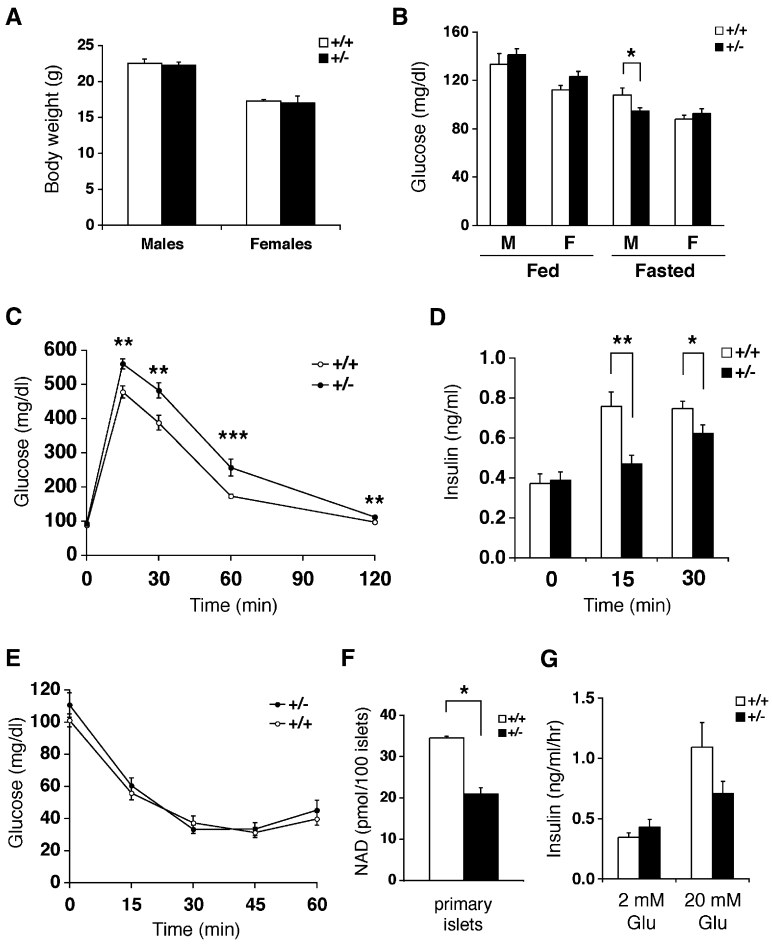

Figure 4. *Nampt*$^{+/-}$ Mice Show Moderately Impaired Glucose Tolerance and Reduced Glucose-Stimulated Insulin Secretion

(A) Body weight of *Nampt*$^{+/-}$ and wild-type (+/+) littermates at 8 weeks of age (n = 7–15).

(B) Fed and fasted glucose levels in male (M) and female (F) *Nampt*$^{+/-}$ and control mice (n = 10–18).

(C) Intraperitoneal glucose tolerance tests (i.p. GTTs). *Nampt*$^{+/-}$ (n = 13) and control (n = 18) females were injected with PBS and fasted for 12–14 hr. Dextrose (3 g/kg body weight) was injected intraperitoneally, and blood glucose levels were measured.

(D) Plasma insulin levels in *Nampt*$^{+/-}$ and control female littermates at 0, 15, and 30 min time points in i.p. GTTs. (n = 14 and 17 for *Nampt*$^{+/-}$ and control mice, respectively, for 0 and 30 min time points; n = 7 and 11 for *Nampt*$^{+/-}$ and control mice, respectively, for 15 min time point.)

(E) Insulin tolerance tests. *Nampt*$^{+/-}$ (n = 9) and control (n = 13) females were injected with human insulin (0.75 U/kg body weight) after fasting for 4 hr, and blood glucose levels were measured.

(F) Nicotinamide adenine dinucleotide (NAD) levels (pmol) in primary islets isolated from *Nampt*$^{+/-}$ and control female mice. NAD levels were measured by HPLC in duplicates of primary islets pooled from three individual mice of each genotype.

(G) Insulin secretion (ng/ml/hr) from *Nampt*$^{+/-}$ and control islets at the indicated glucose concentrations (n = 4 mice for each genotype). Isolated primary islets were cultured overnight in RPMI medium containing 1 μM nicotinamide prior to insulin secretion experiments.

All results are expressed as mean ± SEM. *p ≤ 0.05, **p ≤ 0.01, ***p ≤ 0.001.

notion that *Nampt* haplodeficiency causes defects in NAD biosynthesis and GSIS in pancreatic β cells.

The Defects in *Nampt*$^{+/-}$ Mice and Islets Can Be Corrected by Administering NMN

If the glucose intolerance observed in *Nampt*$^{+/-}$ female mice is indeed due to a lack of the NAD biosynthetic activity of Nampt, administration of NMN, a product of the Nampt enzymatic reaction, might be able to correct their defects. To test this possibility, we used the same *Nampt*$^{+/-}$ and control female cohorts used for the previous i.p. GTTs (see Figure 4C) and injected them intraperitoneally with NMN (500 mg/kg body weight) ~14 hr prior to i.p. GTTs. Interestingly, after NMN administration, there was no difference in blood glucose levels in i.p. GTTs between *Nampt*$^{+/-}$ and control female mice (Figure 5A). In addition, NMN-treated *Nampt*$^{+/-}$ and control mice also had similar plasma insulin levels at each time point (Figure 5B). These data clearly indicate that NMN administration corrects the defect in GSIS observed in *Nampt*$^{+/-}$ mice. We also examined the effect of NMN on GSIS in primary islets isolated from *Nampt*$^{+/-}$ and control female mice that were cultured overnight in RPMI medium containing 1 μM nicotinamide and 50 μM NMN. The addition of NMN significantly augmented insulin secretion in response to 20 mM glucose in both *Nampt*$^{+/-}$ and control islets, and after NMN treatment, GSIS did not differ between *Nampt*$^{+/-}$ and control islets (Figure 5C). These results strongly indicate that the defects observed in *Nampt*$^{+/-}$ mice and islets are due not to a lack of the insulin-mimetic activity of visfatin but rather to a lack of the NAD biosynthetic activity of Nampt.

(SFM), 10 nM insulin (Ins), or 10 nM eNampt/visfatin produced in bacteria (P) or in mammalian cells (E). Signals of phosphorylated proteins were normalized to those of nonphosphorylated proteins, and values are shown relative to the signal in serum-free medium (n ≥ 3).

(E) Insulin receptor phosphorylation was examined in R-IR cells treated with different concentrations of insulin and eNampt/visfatin. Cells were treated with the indicated concentrations of insulin, eNampt/visfatin produced in mammalian cells, or both (10 nM each). InsR was immunoprecipitated with the anti-InsR antibody 29B4 and blotted with an anti-pan-phosphotyrosine antibody (upper panel). The membrane was reprobed with another anti-InsR antibody, C19 (lower panel).

All results are expressed as mean ± SEM.

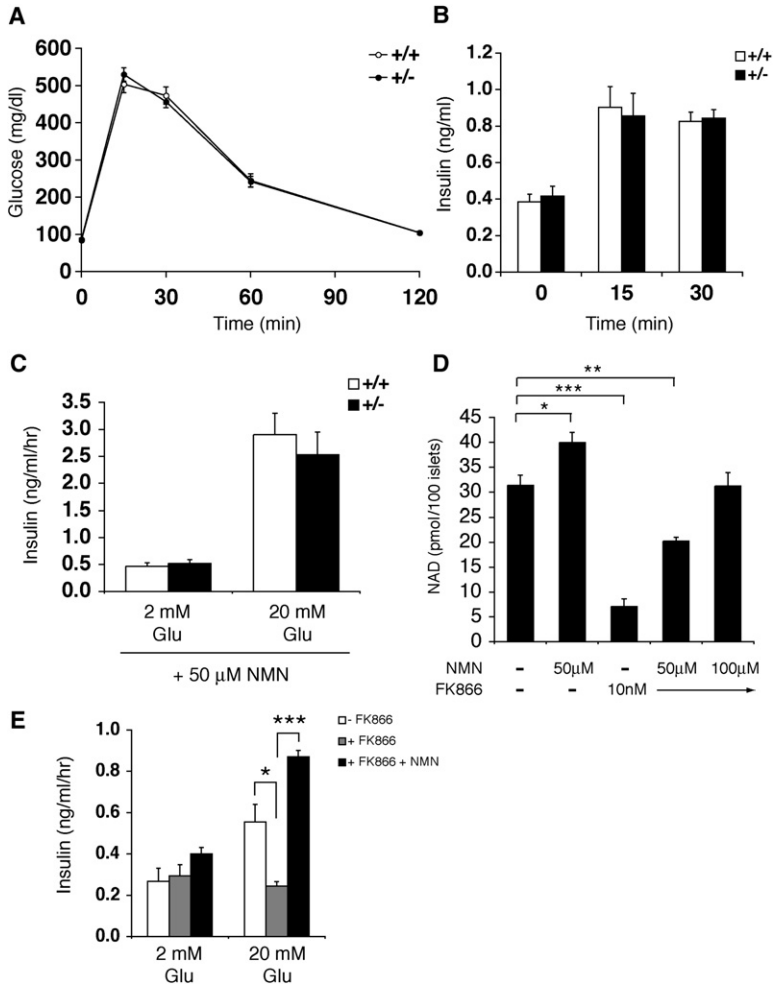

Figure 5. NMN Administration Ameliorates the Defects in *Nampt*$^{+/-}$ Mice and Islets

(A) i.p. GTTs after NMN administration. The same *Nampt*$^{+/-}$ (n = 18) and control (n = 19) cohorts that were used for the i.p. GTTs in Figure 4C were injected with NMN (500 mg/kg body weight) ~14 hr prior to i.p. GTTs.

(B) Plasma insulin levels in *Nampt*$^{+/-}$ and control female littermates at 0, 15, and 30 min time points in i.p. GTTs. (n = 16 and 17 for *Nampt*$^{+/-}$ and control mice, respectively, for 0 and 30 min time points; n = 10 and 8 for *Nampt*$^{+/-}$ and control mice, respectively, for 15 min time point.)

(C) Insulin secretion (ng/ml/hr) from NMN-treated *Nampt*$^{+/-}$ and control islets at the indicated glucose concentrations (n = 4 mice for each genotype). Isolated primary islets were cultured overnight in RPMI medium containing 1 μM nicotinamide plus 50 μM NMN prior to insulin secretion experiments.

(D) NAD levels (pmol) in wild-type primary islets treated overnight with NMN, FK866, or a combination of both at the indicated concentrations. NAD levels were measured by HPLC in triplicates of primary islets pooled from four individual wild-type mice.

(E) Insulin secretion (ng/ml/hr) at the indicated glucose concentrations from control, FK866-treated, and FK866 + NMN-treated wild-type primary islets. Experiments were conducted in triplicates of primary islets pooled from four individual mice cultured for 48 hr in RPMI medium containing 1 μM nicotinamide and the indicated compounds (10 nM for FK866 and 100 μM for NMN) prior to insulin secretion experiments.

All results are expressed as mean ± SEM. *$p \leq 0.05$, **$p \leq 0.01$, ***$p \leq 0.001$.

To further confirm the effect of NMN on NAD biosynthesis and insulin secretion, we measured NAD levels in primary islets cultured overnight with NMN and/or FK866, a potent chemical inhibitor of Nampt (Hasmann and Schemainda, 2003). While 50 μM NMN enhanced NAD biosynthesis by ~30%, 10 nM FK866 inhibited it by ~80% in primary islets (Figure 5D), suggesting that Nampt-mediated NAD biosynthesis is critical for primary islets. Interestingly, in the presence of FK866, the administration of 50–100 μM NMN restored NAD levels in a dose-dependent manner (Figure 5D). Therefore, primary islets are able to use exogenous NMN to maintain normal levels of NAD. GSIS was suppressed by ~60% in primary islets after 48 hr of FK866 treatment, and 100 μM NMN increased insulin secretion in FK866-treated primary islets above control islets (Figure 5E). Taken together, these findings demonstrate that administration of NMN ameliorates defects in NAD biosynthesis and GSIS caused by *Nampt* haplodeficiency or the Nampt inhibitor FK866 in vivo and in vitro.

NMN Circulates Systemically In Blood

eNampt has been reported to be present in human and mouse plasma (Sethi, 2007; Stephens and Vidal-Puig, 2006), and we confirmed this observation by western blotting (Figure S5F). The high NAD biosynthetic activity of eNampt suggests that it might synthesize NMN in blood circulation. Therefore, we tested whether we could detect NMN in mouse plasma by high-pressure liquid chromatography (HPLC). Interestingly, mouse plasma extracts showed a sharp peak at the same elution time as that of standard NMN (Figure 6A). To confirm its identity, we spiked mouse plasma extracts with 100 pmol of NMN and found that the peak of interest was significantly increased (Figure 6B). We also injected NMN (500 mg/kg body weight) into mice and found that the peak of interest increased significantly 15 min after NMN injection (Figure 6C), indicating that this particular peak represents NMN. To further examine the nature of this peak, we collected fractions that contained this peak and analyzed them by ion-trap tandem mass spectrometry. Standard NMN showed the signature *m/z* of 335 and 123 (Figure 6D, upper panel). The same signature spectra of NMN were detected in the peak fractions from mouse plasma extracts (Figure 6D, lower panel), demonstrating that this peak is indeed NMN.

We measured plasma NMN levels by HPLC and calculated its concentrations in control and *Nampt*$^{+/-}$ male and female mice. Wild-type males and females had similar

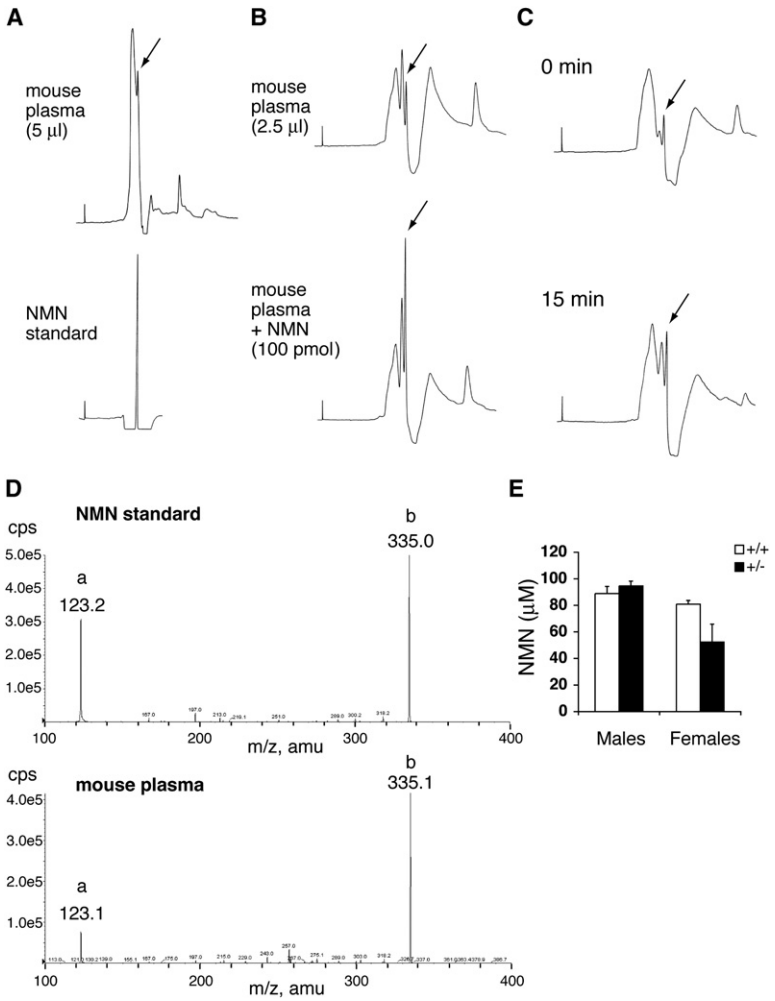

Figure 6. NMN Circulates Systemically in Mouse Blood

(A) HPLC chromatograms of mouse plasma extracts and standard NMN. Extracts that corresponded to 5 μl of plasma and standard NMN were run in an isocratic condition at a flow rate of 1 ml/min. The peak indicated with an arrow shows the same elution time as that of standard NMN.

(B) HPLC chromatograms of mouse plasma extracts with or without a spike of 100 pmol of NMN. Extracts that corresponded to 2.5 μl of plasma were run at a flow rate of 0.7 ml/min. The peaks indicated with arrows showed a significant increase after the NMN spike.

(C) HPLC chromatograms of mouse plasma extracts at 0 and 15 min time points after NMN injection (500 mg/kg body weight). The peaks indicated with arrows showed an increase at the 15 min time point.

(D) Ion-trap tandem mass spectrometry analysis for the fractions containing the peaks indicated with arrows in the HPLC chromatograms. Upper panel, standard NMN; lower panel, the peak fraction of a mouse plasma extract. The signature *m/z* of 123 (a) and 335 (b) for NMN were detected in the peak fraction.

(E) Plasma NMN concentrations in control and *Nampt*$^{+/-}$ male and female mice. Extracts corresponding to 2.5 μl of plasma were analyzed by HPLC, and the NMN peaks were quantitated for control (n = 3) and *Nampt*$^{+/-}$ (n = 4) mice at ~8 months of age. Results are expressed as mean ± SEM.

plasma NMN concentrations (80–90 μM) (Figure 6E). Interestingly, *Nampt*$^{+/-}$ females showed an ~35% decrease in plasma NMN concentrations compared to wild-type littermates, whereas *Nampt*$^{+/-}$ males had values similar to controls (Figure 6E). These sex-related differences are consistent with the differences in plasma eNampt levels between *Nampt*$^{+/-}$ males and females (Figure S5F). This disparity in plasma eNampt and NMN levels between genders is likely the cause of the i.p. GTT defects observed only in *Nampt*$^{+/-}$ females. Taken together, these results clearly demonstrate that NMN, the product of the Nampt enzymatic reaction, circulates systemically in mammalian blood.

DISCUSSION

Nampt/PBEF/Visfatin as an Intra- and Extracellular NAD Biosynthetic Enzyme that Regulates Pancreatic β Cell Function

In this study, we have provided several lines of evidence demonstrating that Nampt functions as an intra- and extracellular NAD biosynthetic enzyme and plays an important role in the regulation of GSIS in pancreatic β cells. First, fully differentiated mouse and human adipocytes produce eNampt. eNampt is positively secreted through a nonclassical secretory pathway, and the presence of eNampt is not due to cell lysis or cell death. Second, eNampt produced by differentiated adipocytes exhibits robust NAD biosynthetic activity that is even higher than iNampt, indicating that Nampt can function as an extracellular enzyme. Third, eNampt does not have any insulin-mimetic activity in vitro or in vivo. Fourth, *Nampt*$^{+/-}$ female mice show impaired glucose tolerance and significantly reduced insulin secretion in i.p. GTTs. Primary islets isolated from *Nampt*$^{+/-}$ mice or treated with FK866 also show significant decreases in NAD biosynthesis and insulin secretion in response to glucose. Fifth, these defects in NAD biosynthesis and GSIS can be corrected by the exogenous administration of NMN in vivo and in vitro. Finally, we have demonstrated that a high concentration of NMN circulates systemically in mouse plasma. These results reveal an important functional mode of Nampt as an extracellular NAD biosynthetic enzyme and strongly support the physiological significance of Nampt-mediated systemic NAD biosynthesis in the regulation of β cell function.

The Physiologically Relevant Function of Secreted eNampt

While the function of iNampt as an essential NAD biosynthetic enzyme is well established (Revollo et al., 2004; Rongvaux et al., 2002; van der Veer et al., 2005), the physiological role of eNampt remains controversial. In this study, we attempted to reproduce the reported insulin-mimetic effects of eNampt/visfatin on adipogenesis, glucose uptake, cellular insulin signaling, and blood glucose levels in mice. Surprisingly, we were unable to obtain evidence supporting the insulin-mimetic activity of eNampt/visfatin. Furthermore, we found that *Nampt*$^{+/-}$ mice and islets have defects in NMN/NAD biosynthesis and GSIS. These defects are ameliorated by NMN administration in *Nampt*$^{+/-}$ mice and islets. Thus, these findings strongly indicate that the defects observed in *Nampt*$^{+/-}$ mice and islets are due not to a lack of the proposed insulin-mimetic activity of visfatin but to a lack of Nampt-catalyzed NMN production. This conclusion is also supported by the findings that the chemical inhibition of Nampt by FK866 also causes defects in NAD biosynthesis and GSIS in primary islets and that these defects are ameliorated by exogenous NMN administration. Therefore, we conclude that it is the NAD biosynthetic activity of Nampt, not the insulin-mimetic activity of visfatin, that is physiologically important for the regulation of glucose metabolism.

Cell-Type-Dependent Regulation of eNampt Secretion

The fact that eNampt is positively secreted through a nonclassical secretory pathway in a cell-type-dependent manner indicates that the secretion of eNampt is a highly regulated process. Because Nampt-FLAG has different enzymatic activities dependent on the cell type and the compartment, it is very likely that a posttranslational modification is responsible for one or both of the altered enzymatic activity and the secretion of eNampt. The treatment of eNampt-FLAG from HIB-1B conditioned medium with calf intestinal phosphatase and N-acetylglucosaminidase did not change its enzymatic activity (data not shown), and an extensive mass spectrometric search for the modification has so far been unsuccessful. Further investigation will be necessary to identify the presumed modification of eNampt.

Interestingly, adipocytes apparently acquire the ability to modify and secrete Nampt during their differentiation process. Among the several cell types examined, only fully differentiated adipocytes naturally produce eNampt. Thus, it is conceivable that adipose tissue might be one of the major sites of eNampt production in vivo. Under normal physiological conditions, WAT does not appear to produce high levels of iNampt and eNampt. However, in certain pathophysiological conditions that cause significant changes in adipose tissue mass, structure, and/or function, such as obesity and type 2 diabetes, WAT might secrete more eNampt. Indeed, it has been reported that circulating levels of eNampt are increased by hyperglycemia (Haider et al., 2006b). Additionally, there are several clinical studies reporting that higher plasma eNampt levels

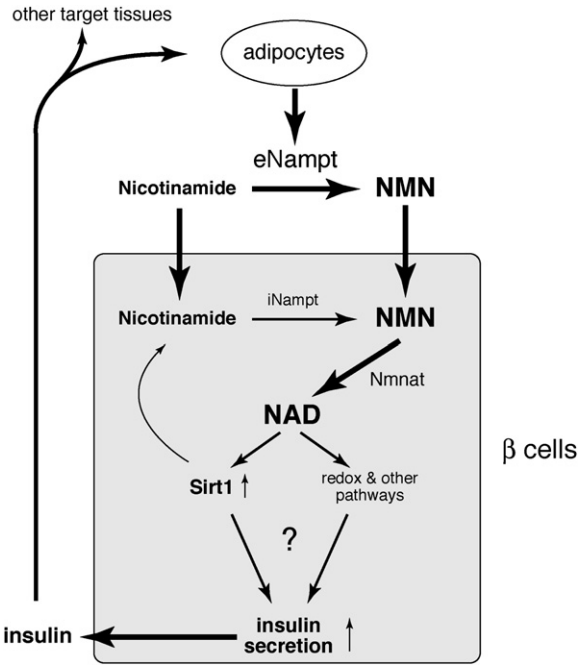

Figure 7. A Model for the Regulation of Insulin Secretion by Nampt-Mediated Systemic NAD Biosynthesis in Pancreatic β Cells

See text for details. eNampt, extracellular Nampt; iNampt, intracellular Nampt; NMN, nicotinamide mononucleotide; Nmnat, nicotinamide/nicotinic acid mononucleotide adenylyltransferase.

are associated with higher body mass index and percent body fat (Berndt et al., 2005), type 2 diabetes (Chen et al., 2006), and obesity in children (Haider et al., 2006a). Therefore, it will be of great importance to identify the stimuli that cause increased production of eNampt in white adipocytes in these pathophysiological conditions.

Nampt-Mediated Systemic NAD Biosynthesis and Its Importance in the Regulation of Glucose Metabolism

The findings that eNampt possesses robust NAD biosynthetic activity and that 80–90 μM NMN circulates in mouse plasma are striking, as it has been thought that NAD biosynthesis is an entirely intracellular process (Magni et al., 1999; Rongvaux et al., 2003). Interestingly, only *Nampt*$^{+/-}$ females, but not males, have reduced plasma levels of eNampt and NMN as well as defects in glucose metabolism. Although it is currently unclear why and how *Nampt*$^{+/-}$ males maintain their plasma eNampt and NMN levels, these results suggest that the maintenance of high NMN levels by eNampt in blood circulation is critical for normal β cell function, probably because pancreatic islets have very low levels of iNampt compared to other tissues. Furthermore, NMN concentrations in wild-type mouse plasma are within the range that can enhance and restore NAD biosynthesis and GSIS in normal and FK866-treated primary islets in vitro, respectively. Based on these findings, we propose that NMN functions as an

essential plasma metabolite that can modulate pancreatic β cell function (Figure 7). Given that fully differentiated adipocytes are natural producers of eNampt, adipose tissue may regulate β cell function through secretion of eNampt and extracellular biosynthesis of NMN (Figure 7). Intriguingly, individuals homozygous for either of two single-nucleotide polymorphism variants in the *Nampt* gene promoter region have lower fasting plasma insulin levels (Bailey et al., 2006). Therefore, circulating NMN levels, maintained by plasma eNampt, may play an important role in regulating β cell function in physiological and pathophysiological conditions. It will be of great interest to measure eNampt activity and NMN levels in plasma samples from patients with obesity and/or type 2 diabetes by developing high-throughput detection methods.

Although the molecular mechanism underlying attenuated GSIS in $Nampt^{+/-}$ islets is still unclear, alterations in NAD levels could alter activities of important enzymes in metabolic pathways such as glycolysis or fatty acid oxidation in pancreatic β cells (Figure 7). These changes in NAD would also affect other NAD-dependent enzymes, such as the NAD-dependent deacetylase Sirt1 or poly-ADP-ribose polymerase (PARP) (Figure 7). Sirt1 is particularly interesting in this regard because we have previously demonstrated that it promotes GSIS in β cells using pancreatic β cell-specific Sirt1-overexpressing (BESTO) mice (Moynihan et al., 2005). Interestingly, the phenotypes observed in BESTO mice are the opposite of those observed in $Nampt^{+/-}$ mice. Furthermore, NMN administration can also augment GSIS in aged BESTO mice (K.F.M. and S.I., unpublished data), suggesting that Sirt1 is a downstream regulator in pancreatic β cells that responds to alterations in systemic NAD biosynthesis. Although further investigation will be necessary to test the model, the discovery that Nampt-mediated systemic NAD biosynthesis is a critical contributor to β cell function opens up important avenues for the development of therapeutics to treat metabolic diseases such as type 2 diabetes.

EXPERIMENTAL PROCEDURES

Detection of Intracellular Nampt in Tissues

Ad libitum-fed C57BL/6 mice aged 3–4 months were sacrificed by carbon dioxide asphyxiation. Organs were immediately collected, homogenized in 1× Laemmli SDS sample buffer, and boiled for 5 min. Samples were then centrifuged at 20,000 × g to remove debris, and protein concentrations were measured by Bradford assay (Bio-Rad). 22.5 μg tissue extracts were analyzed by western blotting with a rabbit polyclonal anti-Nampt antibody as described previously (Revollo et al., 2004).

Differentiation of 3T3-L1, HIB-1B, and SGBS Preadipocyte Cell Lines

All mouse cell lines were cultured in Dulbecco's modified Eagle's medium supplemented with 10% fetal bovine serum and antibiotics. Confluent cultures of HIB-1B brown preadipocytes were differentiated by adding 5 μg/ml insulin, 0.5 mM isobutylmethylxanthine (IBMX), 1 μM dexamethasone, and 1 nM triiodothyronine (T3, Sigma) for 2 days and then refeeding the medium containing 5 μg/ml insulin and 1 nM T3 every other day for 6 more days. 3T3-L1 white preadipocytes were differentiated similarly, except that T3 was absent from the medium throughout the entire differentiation process.

Human SGBS preadipocytes (Wabitsch et al., 2001), kindly provided by M. Wabitsch (University of Ulm, Germany), were grown and differentiated into mature adipocytes as described previously (Körner et al., 2005). Briefly, preadipocytes at confluence were exposed to serum-free basal medium supplemented with 10 μg/ml apotransferrin, 20 nM human recombinant insulin, 10 nM hydrocortisone, and 0.2 nM triiodothyroxine. For the first 4 days, this adipocyte culture medium was additionally supplemented with 25 nM dexamethasone, 500 μM IBMX, and 2 μM rosiglitazone.

iNampt and eNampt proteins were detected by western blotting with whole-cell extracts or culture supernatants and anti-Nampt antibodies. A rabbit polyclonal antibody (Revollo et al., 2004) and a mouse monoclonal antibody (OMNI379, ALX-804-717, Axxora) were used for these experiments.

Expression and Immunoprecipitation of Intra- and Extracellular Nampt-FLAG

A C-terminally FLAG-tagged mouse Nampt (Nampt-FLAG) cDNA was created with the following forward and reverse primers containing EcoRI sites: forward, 5′-TTAGAATTCAGCCCATTTTTCTCCTTGCT-3′; reverse, 5′-AATGAATTCTACTTATCGTCGTCATCCTTGTAATCTCCTC CATGAGGTGCCACGTCCTGCTCGATGTT-3′. The resulting cDNA was confirmed by sequencing. The Nampt-FLAG cDNA was then cloned into the mammalian expression vector pCXN2. To create HIB-1B cell lines expressing Nampt-FLAG, HIB-1B cells were transfected with pCXN2-Nampt-FLAG or pCXN2 and selected at 500 μg/ml of G418 (Invitrogen, CA) for 2 weeks.

For immunoprecipitation of intracellular Nampt-FLAG, whole-cell extracts were prepared with ice-cold immunoprecipitation (IP) buffer (phosphate-buffered saline [pH 7.4], 0.5% NP-40, 1 mM EDTA, 1 mM NaF, 10 μM trichostatin A, 10 mM nicotinamide, 0.5 mM DTT, protease inhibitor cocktail [Roche]) and mixed with agarose beads conjugated with mouse monoclonal M2 anti-FLAG antibody (F2426, Sigma) for 3–4 hours at 4°C. For immunoprecipitation of extracellular Nampt-FLAG, HIB-1B culture supernatants were collected after incubating differentiated HIB-1B cells overnight with DMEM without fetal bovine serum but supplemented with 1 μg/ml insulin and 1 nM triiodothyronine, filtered through a 0.22 μm PES membrane, concentrated with Amicon Ultra-15 columns (Millipore), and mixed with anti-FLAG beads for 3–4 hours at 4°C. Immunoprecipitates were washed twice with IP buffer and twice with PBS.

Enzymatic Reactions

Nampt enzymatic reactions were conducted as previously described (Revollo et al., 2004). Briefly, immunoprecipitates on anti-FLAG beads were incubated in enzymatic reaction buffer (50 mM Tris-HCl [pH 8.5], 100 mM NaCl, 0.25 mM nicotinamide, 10 mM $MgSO_4$, 1.5% ethanol, 0.5 mM PRPP, 2.0 mM ATP) for 55 min at 37°C. After this reaction, mouse recombinant Nmnat and yeast alcohol dehydrogenase (Sigma) were added at a final concentration of 10 μg/ml each, and the mixture was incubated for 5 min at 37°C. Supernatants were then collected by spinning down anti-FLAG beads, and autofluorescence of NADH was measured in a PerkinElmer LS 50B fluorometer (340 nm excitation, 460 nm emission). NADH autofluorescence values were converted to the amounts of NMN using the standard curve drawn with known amounts of NMN. Immunoprecipitates bound on anti-FLAG beads were extracted with Laemmli sample buffer, boiled for 5 minutes, and analyzed by western blotting with anti-Nampt antibodies. The amounts of Nampt used for enzymatic reactions were quantitated compared to the standards of mouse recombinant Nampt. k_{cat} values were calculated based on the molar amount of NMN generated per the molar amount of immunoprecipitated Nampt-FLAG protein per unit time.

eNampt Secretion Assays

C-terminally FLAG-tagged versions of mouse dihydrofolate reductase (Dhfr, a gift from W. Yokoyama, Washington University) and bovine preprolactin (Ppl, a gift from C. Nicchitta, Duke University) were

created as intracellular and extracellular protein controls (pCXN2-Dhfr-FLAG and pCXN2-Ppl-FLAG), respectively, and HIB-1B preadipocyte cell lines stably expressing these proteins were generated.

HIB-1B cells expressing Nampt-FLAG, Dhfr-FLAG, and Ppl-FLAG were differentiated as described above. To detect intracellular FLAG-tagged proteins, cell extracts were collected and immunoprecipitated as described above. To detect extracellular FLAG-tagged proteins, culture supernatants (~8 ml) were collected, immunoprecipitated overnight at 4°C with anti-FLAG antibody-conjugated beads, and analyzed by western blotting with rabbit polyclonal anti-FLAG antibody (Sigma). For the BFA experiment, cells were treated with BFA (0.5 μg/ml, Sigma) for 12 hr.

CHO cells at 50%–60% confluency were transfected with pCXN2, pCXN2-Dhfr-FLAG, pCXN2-Ppl-FLAG, or pCXN2-Nampt-FLAG. Cell extracts and culture supernatants were collected 48 hr after transfection, subjected to immunoprecipitation with anti-FLAG antibody-conjugated beads, and analyzed by western blotting as described above.

Glucose and Insulin Measurements

Glucose levels were determined using an Accu-Chek II glucometer (Roche Diagnostics) with blood collected from the tail vein. For determining insulin levels, blood was collected from the tail vein in chilled heparinized capillary tubes, and plasma was separated by centrifugation and stored at −80°C. Insulin levels were determined on 5–10 μl aliquots using a rat insulin ELISA kit with mouse insulin standards (ALPCO) at the Washington University RIA Core Facility.

Intraperitoneal Glucose Tolerance Tests and Insulin Tolerance Tests

For i.p. GTTs, mice were injected with PBS or NMN (500 mg/kg body weight) and fasted for 14 hrs; dextrose (3 g/kg body weight) was then injected intraperitoneally; and blood glucose levels were measured at 0, 15, 30, 60, and 120 min after injection. Plasma was also collected at 0, 15, and 30 min time points after glucose injection and submitted to the Washington University RIA Core Facility for insulin measurements. For insulin tolerance tests, female mice were fasted for 4 hrs; human insulin (0.75 U/kg body weight; Lilly) was injected intraperitoneally; and blood glucose levels were measured at 0, 15, 30, 45, and 60 min after insulin injection. All animal procedures were approved by the Washington University Animal Studies Committee.

Glucose-Stimulated Insulin Secretion from Primary Islets

Islets were isolated by collagenase digestion as described previously (Moynihan et al., 2005). Briefly, pancreata were inflated with isolation buffer (10× HBSS, 10 mM HEPES, 1 mM $MgCl_2$, 5 mM glucose [pH 7.4]) containing 0.375 mg/ml collagenase (Sigma) via the pancreatic duct after clamping off its entry site to the duodenum. The inflated pancreata were then removed, incubated at 37°C for 12–15 min, and shaken vigorously. Islets were separated from acinar tissue after a series of washes and passages through a 70 μm nylon BD Falcon Cell Strainer (BD Biosciences). Hand-picked islets were cultured overnight in RPMI medium containing 1 μM nicotinamide, 5 mM glucose, 2 mM L-glutamine, penicillin/streptomycin, and 10% fetal bovine serum. The islets were then preincubated in oxygenated Krebs-Ringer bicarbonate (KRB) buffer (1 μM nicotinamide, 119 mM NaCl, 4.7 mM KCl, 25 mM $NaHCO_3$, 2.5 mM $CaCl_2$, 1.2 mM $MgSO_4$, 1.2 mM KH_2PO_4, and 0.25% radioimmunoassay-grade BSA) supplemented with 2 mM glucose for 1 hr at 37°C. Islets of similar size were hand picked into groups of ten islets in triplicate and incubated with 1 ml KRB buffer containing either 2 mM glucose or 20 mM glucose for 1 hr at 37°C.

For treatments with NMN, FK866, or the combination of the two compounds, primary islets were pooled from three or four wild-type B6 mice and grouped for each experimental condition. Islets were cultured overnight or for up to 48 hr in RPMI media containing 50–100 μM NMN and/or 10 nM FK866 prior to insulin secretion experiments.

Statistical Analyses

Statistical analyses were carried out using an unpaired Student's t test. All values are expressed as mean ± standard error of the mean (SEM). Differences were considered to be statistically significant when $p \leq 0.05$.

For additional experimental procedures, see Supplemental Data.

Supplemental Data

Supplemental Data include Supplemental Experimental Procedures, Supplemental References, six figures, and one table and can be found with this article online at http://www.cellmetabolism.org/cgi/content/full/6/5/363/DC1/.

ACKNOWLEDGMENTS

We thank P. Bickel for 3T3-L1 and HIB-1B cells, W. Yokoyama and C. Nicchitta for *Dhfr* and *Ppl* cDNAs respectively, G. Gokel for a fluorometer, G.W. Sherrow for insulin measurements, M. Case for mass spectrometry analysis, and R. Tauscher and A. Berthold for technical assistance. We also thank N. Abumrad, I. Boime, J. Shaffer, and T. Baranski for critical comments and suggestions and the members of the Imai and Kiess labs for their help and encouragement. J.R.R. is a fellow supported by the Lucille P. Markey Special Emphasis Pathway in Human Pathology. A.K. and W.K. are supported by grants from the Deutsche Forschungsgemeinschaft KFO152: "Atherobesity" projects BE 1264/10-1 (to W.K.) and KO 3512/1-1 (to A.K), the Translational Centre for Regenerative Medicine (project 1082MN), and the German Diabetes Association (to A.K.). J.M. is supported by grants from the Muscular Dystrophy Association and National Institutes of Health (NS36358). R.R.T. is supported in part by the National Center for Research Resources (P41RR00945) and National Institute of Diabetes and Digestive and Kidney Diseases (P30 DK52574). S.I. is an Ellison Medical Foundation Scholar in Aging and is also supported by grants from the National Institute on Aging (AG024150), American Diabetes Association, Juvenile Diabetes Research Foundation, Washington University Clinical Nutrition Research Unit (DK56341), and the National Center for Research Resources (C06RR015502). J.M. and C.W. are members of the scientific advisory board of Sirtris Pharmaceuticals, Inc. S.I. and J.R.R. are holders of intellectual property rights regarding the uses of Nampt and NMN, one of which is licensed to Sirtris Pharmaceuticals, Inc.

Received: April 3, 2007
Revised: July 31, 2007
Accepted: September 12, 2007
Published: November 6, 2007

REFERENCES

Arner, P. (2006). Visfatin–a true or false trail to type 2 diabetes mellitus. J. Clin. Endocrinol. Metab. *91*, 28–30.

Bailey, S.D., Loredo-Osti, J.C., Lepage, P., Faith, J., Fontaine, J., Desbiens, K.M., Hudson, T.J., Bouchard, C., Gaudet, D., Perusse, L., et al. (2006). Common polymorphisms in the promoter of the visfatin gene (PBEF1) influence plasma insulin levels in a French-Canadian population. Diabetes *55*, 2896–2902.

Belenky, P., Bogan, K.L., and Brenner, C. (2007). NAD^+ metabolism in health and disease. Trends Biochem. Sci. *32*, 12–19.

Berndt, J., Kloting, N., Kralisch, S., Kovacs, P., Fasshauer, M., Schon, M.R., Stumvoll, M., and Bluher, M. (2005). Plasma visfatin concentrations and fat depot-specific mRNA expression in humans. Diabetes *54*, 2911–2916.

Chen, M.P., Chung, F.M., Chang, D.M., Tsai, J.C., Huang, H.F., Shin, S.J., and Lee, Y.J. (2006). Elevated plasma level of visfatin/pre-B cell colony-enhancing factor in patients with type 2 diabetes mellitus. J. Clin. Endocrinol. Metab. *91*, 295–299.

Denu, J.M. (2003). Linking chromatin function with metabolic networks: Sir2 family of NAD(+)-dependent deacetylases. Trends Biochem. Sci. *28*, 41–48.

Fukuhara, A., Matsuda, M., Nishizawa, M., Segawa, K., Tanaka, M., Kishimoto, K., Matsuki, Y., Murakami, M., Ichisaka, T., Murakami, H., et al. (2005). Visfatin: a protein secreted by visceral fat that mimics the effects of insulin. Science *307*, 426–430.

Haider, D.G., Holzer, G., Schaller, G., Weghuber, D., Widhalm, K., Wagner, O., Kapiotis, S., and Wolzt, M. (2006a). The adipokine visfatin is markedly elevated in obese children. J. Pediatr. Gastroenterol. Nutr. *43*, 548–549.

Haider, D.G., Schaller, G., Kapiotis, S., Maier, C., Luger, A., and Wolzt, M. (2006b). The release of the adipocytokine visfatin is regulated by glucose and insulin. Diabetologia *49*, 1909–1914.

Hasmann, M., and Schemainda, I. (2003). FK866, a highly specific noncompetitive inhibitor of nicotinamide phosphoribosyltransferase, represents a novel mechanism for induction of tumor cell apoptosis. Cancer Res. *63*, 7436–7442.

Hug, C., and Lodish, H.F. (2005). Medicine. Visfatin: a new adipokine. Science *307*, 366–367.

Imai, S., Armstrong, C.M., Kaeberlein, M., and Guarente, L. (2000). Transcriptional silencing and longevity protein Sir2 is an NAD-dependent histone deacetylase. Nature *403*, 795–800.

Jia, S.H., Li, Y., Parodo, J., Kapus, A., Fan, L., Rotstein, O.D., and Marshall, J.C. (2004). Pre-B cell colony-enhancing factor inhibits neutrophil apoptosis in experimental inflammation and clinical sepsis. J. Clin. Invest. *113*, 1318–1327.

Khan, J.A., Tao, X., and Tong, L. (2006). Molecular basis for the inhibition of human NMPRTase, a novel target for anticancer agents. Nat. Struct. Mol. Biol. *13*, 582–588.

Kim, M.K., Lee, J.H., Kim, H., Park, S.J., Kim, S.H., Kang, G.B., Lee, Y.S., Kim, J.B., Kim, K.K., Suh, S.W., and Eom, S.H. (2006). Crystal structure of visfatin/pre-B cell colony-enhancing factor 1/nicotinamide phosphoribosyltransferase, free and in complex with the anti-cancer agent FK-866. J. Mol. Biol. *362*, 66–77.

Körner, A., Wabitsch, M., Seidel, B., Fischer-Posovszky, P., Berthold, A., Stumvoll, M., Bluher, M., Kratzsch, J., and Kiess, W. (2005). Adiponectin expression in humans is dependent on differentiation of adipocytes and down-regulated by humoral serum components of high molecular weight. Biochem. Biophys. Res. Commun. *337*, 540–550.

Landry, J., Slama, J.T., and Sternglanz, R. (2000). Role of NAD^+ in the deacetylase activity of the SIR2-like proteins. Biochem. Biophys. Res. Commun. *278*, 685–690.

Lin, S.-J., and Guarente, L. (2003). Nicotinamide adenine dinucleotide, a metabolic regulator of transcription, longevity and disease. Curr. Opin. Cell Biol. *15*, 241–246.

Magni, G., Amici, A., Emanuelli, M., Raffaelli, N., and Ruggieri, S. (1999). Enzymology of NAD+ synthesis. Adv. Enzymol. Relat. Areas Mol. Biol. *73*, 135–182.

Magni, G., Amici, A., Emanuelli, M., Orsomando, G., Raffaelli, N., and Ruggieri, S. (2004). Enzymology of NAD+ homeostasis in man. Cell. Mol. Life Sci. *61*, 19–34.

Martin, P., Shea, R., and Mulks, M. (2001). Identification of a plasmid-encoded gene from *Haemophilus ducreyi* which confers NAD independence. J. Bacteriol. *183*, 1168–1174.

Miller, E.S., Heidelberg, J.F., Eisen, J.A., Nelson, W.C., Durkin, A.S., Ciecko, A., Feldblyum, T.V., White, O., Paulsen, I.T., Nierman, W.C., et al. (2003). Complete genome sequence of the broad-host-range vibriophage KVP40: comparative genomics of a T4-related bacteriophage. J. Bacteriol. *185*, 5220–5233.

Miura, M., Surmacz, E., Burgaud, J.L., and Baserga, R. (1995). Different effects on mitogenesis and transformation of a mutation at tyrosine 1251 of the insulin-like growth factor I receptor. J. Biol. Chem. *270*, 22639–22644.

Moschen, A.R., Kaser, A., Enrich, B., Mosheimer, B., Theurl, M., Niederegger, H., and Tilg, H. (2007). Visfatin, an adipocytokine with proinflammatory and immunomodulating properties. J. Immunol. *178*, 1748–1758.

Moynihan, K.A., Grimm, A.A., Plueger, M.M., Bernal-Mizrachi, E., Ford, E., Cras-Meneur, C., Permutt, M.A., and Imai, S. (2005). Increased dosage of mammalian Sir2 in pancreatic β cells enhances glucose-stimulated insulin secretion in mice. Cell Metab. *2*, 105–117.

Ognjanovic, S., and Bryant-Greenwood, G.D. (2002). Pre-B-cell colony-enhancing factor, a novel cytokine of human fetal membranes. Am. J. Obstet. Gynecol. *187*, 1051–1058.

Revollo, J.R., Grimm, A.A., and Imai, S. (2004). The NAD biosynthesis pathway mediated by nicotinamide phosphoribosyltransferase regulates Sir2 activity in mammalian cells. J. Biol. Chem. *279*, 50754–50763.

Revollo, J.R., Grimm, A.A., and Imai, S. (2007). The regulation of nicotinamide adenine dinucleotide biosynthesis by Nampt/PBEF/visfatin in mammals. Curr. Opin. Gastroenterol. *23*, 164–170.

Rongvaux, A., Andris, F., Van Gool, F., and Leo, O. (2003). Reconstructing eukaryotic NAD metabolism. Bioessays *25*, 683–690.

Rongvaux, A., Shea, R.J., Mulks, M.H., Gigot, D., Urbain, J., Leo, O., and Andris, F. (2002). Pre-B-cell colony-enhancing factor, whose expression is up-regulated in activated lymphocytes, is a nicotinamide phosphoribosyltransferase, a cytosolic enzyme involved in NAD biosynthesis. Eur. J. Immunol. *32*, 3225–3234.

Samal, B., Sun, Y., Stearns, G., Xie, C., Suggs, S., and McNiece, I. (1994). Cloning and characterization of the cDNA encoding a novel human pre-B-cell colony-enhancing factor. Mol. Cell. Biol. *14*, 1431–1437.

Sethi, J.K. (2007). Is PBEF/visfatin/Nampt an authentic adipokine relevant to the metabolic syndrome? Curr. Hypertens. Rep. *9*, 33–38.

Smith, J.S., Brachmann, C.B., Celic, I., Kenna, M.A., Muhammad, S., Starai, V.J., Avalos, J.L., Escalante-Semerena, J.C., Grubmeyer, C., Wolberger, C., and Boeke, J.D. (2000). A phylogenetically conserved NAD^+-dependent protein deacetylase activity in the Sir2 protein family. Proc. Natl. Acad. Sci. USA *97*, 6658–6663.

Stephens, J.M., and Vidal-Puig, A.J. (2006). An update on visfatin/pre-B cell colony-enhancing factor, an ubiquitously expressed, illusive cytokine that is regulated in obesity. Curr. Opin. Lipidol. *17*, 128–131.

van der Veer, E., Nong, Z., O'Neil, C., Urquhart, B., Freeman, D., and Pickering, J.G. (2005). Pre-B-cell colony-enhancing factor regulates NAD^+-dependent protein deacetylase activity and promotes vascular smooth muscle cell maturation. Circ. Res. *97*, 25–34.

Wabitsch, M., Brenner, R.E., Melzner, I., Braun, M., Moller, P., Heinze, E., Debatin, K.M., and Hauner, H. (2001). Characterization of a human preadipocyte cell strain with high capacity for adipose differentiation. Int. J. Obes. Relat. Metab. Disord. *25*, 8–15.

Wang, B., Jenkins, J.R., and Trayhurn, P. (2005). Expression and secretion of inflammation-related adipokines by human adipocytes differentiated in culture: integrated response to TNF-alpha. Am. J. Physiol. Endocrinol. Metab. *288*, E731–E740.

Wang, T., Zhang, X., Bheda, P., Revollo, J.R., Imai, S., and Wolberger, C. (2006). Structure of Nampt/PBEF/visfatin, a mammalian NAD(+) biosynthetic enzyme. Nat. Struct. Mol. Biol. *13*, 661–662.

Ye, S.Q., Simon, B.A., Maloney, J.P., Zambelli-Weiner, A., Gao, L., Grant, A., Easley, R.B., McVerry, B.J., Tuder, R.M., Standiford, T., et al. (2005). Pre-B-cell colony-enhancing factor as a potential novel biomarker in acute lung injury. Am. J. Respir. Crit. Care Med. *171*, 361–370.